Quantum Electronics **46** (12) 1134–1138 (2016)

DOI: 10.1070/QEL16224

Multicore optical fibre and fibre-optic delay line based on it

O.N. Egorova, M.S. Astapovich, M.E. Belkin, S.L. Semjonov

Abstract. **The first switchable fibre-optic delay line based on a 1300-m-long multicore optical fibre has been fabricated and investigated. We have obtained signal delay times of up to 45 μs at 6.43-μs intervals. Sequential signal propagation through the cores of the multicore optical fibre makes it possible to reduce the fibre length necessary for obtaining a predetermined delay time, which is important for reducing the weight and dimensions of devices based on the use of fibre-optic delay lines.**

Keywords: *multicore optical fibre, group delay, fibre-optic delay lines.*

1. Introduction

Microwave signal processing, generation and transmission with the help of light constitute an interdisciplinary area of research referred to as microwave photonics [1, 2]. In most microwave photonics applications, an analog microwave signal is converted to the optical range by modulating highly coherent optical light. For further processing of such a modulated optical signal, wide use is made of various types of multichannel and single-channel delay lines, which are key elements of microwave photonics devices [3, 4]. A number of applications require lines that ensure a considerable signal delay (longer than 100 μs). Devices that ensure such signal delays are include fibre-optic delay lines (FODLs).

In FODLs, a delay of an optical signal modulated by a microwave signal is ensured by propagation through a single-mode fibre segment of length L. The delay time is $\tau = Ln_g/c$, where n_g is the mode group index of the fibre and c is the speed of light in vacuum. FODLs offer a number of advantages over their electronic analogues: simple design, good electromagnetic interference resistance, low noise and insignificant cross-talk between signals. Their main drawback is the large dimensions and weight necessary for obtaining delay times of 100 μs and longer, because considerable lengths of fibre are then needed. Large dimensions and weight of microwave signal processing devices are unacceptable, especially in on-board communication applications.

O.N. Egorova, M.S. Astapovich, S.L. Semjonov Fiber Optics Research Center, Russian Academy of Sciences, ul. Vavilova 38, 119333 Moscow, Russia; e-mail: egorova@fo.gpi.ru;
M.E. Belkin Moscow Technological University (Moscow Institute of Radio Engineering, Electronics and Automation), prosp. Vernadskogo 78, 119454 Moscow, Russia

Received 30 September 2016; revision received 21 October 2016
Kvantovaya Elektronika **46** (12) 1134–1138 (2016)
Translated by O.M. Tsarev

The dimensions and weight of FODLs can be reduced by using a multicore fibre (MCF) [5], having not one but several cores. Since an optical signal sequentially passes through each core of an MCF, a required delay can be ensured at an MCF length equal to the length of an appropriate single-core fibre divided by the number of cores in the MCF [6]. In this paper, we report the fabrication and parameters of a multicore fibre-based switchable fibre-optic delay line. Practical implementation of such delay line design has not yet been reported in the literature.

2. MCF-based FODL configuration

Figure 1 shows a schematic of the MCF-based switchable FODL with input/output (IO) devices connected to it on both sides. The signal source used was a highly coherent semiconductor laser (SL) emitting at a wavelength of 1550.92 nm. To model a microwave signal, we used a signal generator (SG) that produced a train of 1-μs microwave pulses with a repetition rate of 50 μs and carrier frequency of 100 MHz. The SL output was modulated by the signal from the SG using an electro-optical modulator (EOM). After the EOM, the modulated light was sent to a micro-optical electromechanical switch (S1). In one position of S1, the signal was fed to a zero signal delay channel, i.e. to a short single-core fibre segment. In the other position of S1, the signal was launched into a single-core fibre and then into the first core (C1) of the MCF through an input/output device (IO1), which coupled the light into one of the MCF cores and then coupled it out of the core and into a single-core fibre. Propagating through C1, the signal acquired a time delay $\tau = Ln_g/c$. After that, switch S2 directed it to either the FODL output or the next core (C2). The MCF length was 1300 m. At $n_g = 1.468$ (telecom fibre), the calculated τ after propagation through one core was 6.36 μs. After propagation through C2, the time delay of the signal was 2τ and it was directed by S3 to either the output of the delay line or the third core (C3). Time delays of 3τ, 4τ, 5τ, 6τ and 7τ could be obtained in a similar manner. At the FODL output, the different channels were combined using an 8×1 fibre-optic summation unit. Thus, at each instant of time, the signal in the MCF-based switchable delay line configuration under study had a time delay from zero to 7τ, with a constant interval τ.

The output signal from the optical summation unit was converted into an electrical signal by a photodetector (PD), whose output was fed to a broadband oscilloscope (BO). To determine the delay time, a synchronisation signal corresponding to the instant when the leading edge of the modulating microwave pulse arrived at the EOM input was also sent from the SG to the oscilloscope input.

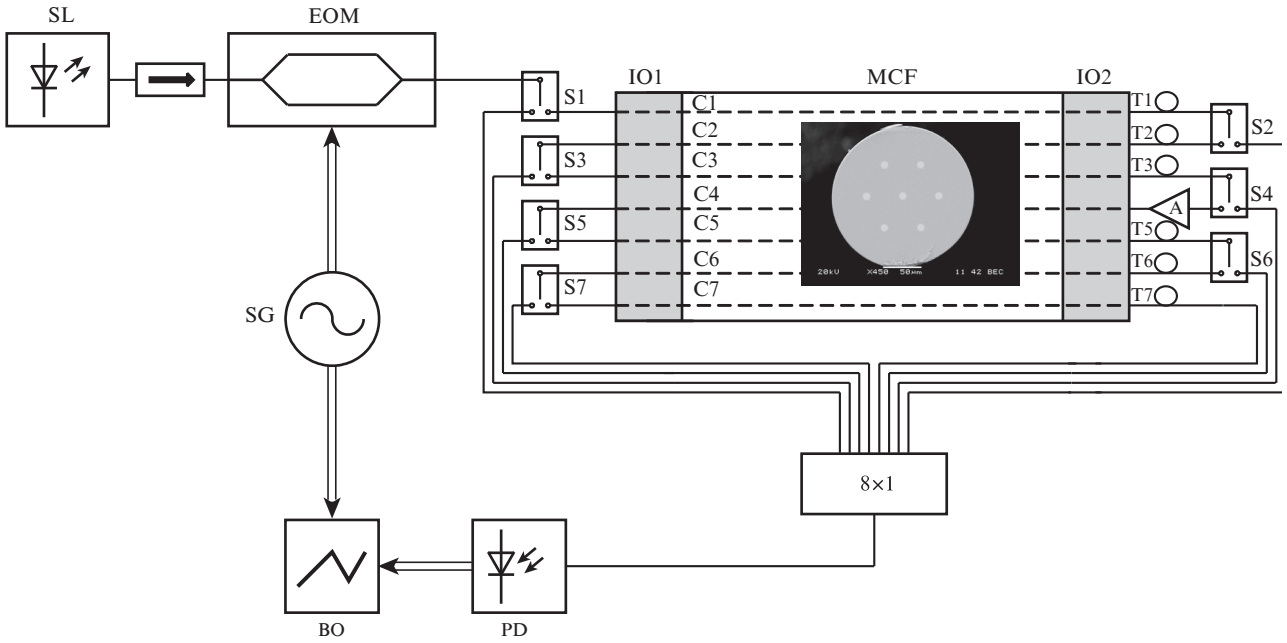

Figure 1. Schematic of the MCF-based delay line (T1–T7, additional turns; A, amplifier). Inset: cross-sectional photograph of the MCF.

3. Multicore optical fibre for the FODL

The use of a seven-core fibre instead of a single-core one in the above scheme enables a sevenfold reduction in the fibre length necessary for obtaining a required signal delay. The delay line includes seven channels, which ensure identical optical signal delays. The optical paths in the channels (between switches S1 and S2, S2 and S3 etc.) can be equalised by adjusting the length of the lead-in single-core fibres, but it is desirable that all the cores in the MCF segment have identical optical lengths. Because of this, the FODL was produced using an MCF with identical parameters of its cores and, hence, with identical mode group indices of neighbouring cores.

The MCF was produced by drilling [7]. To this end, holes were drilled in a 20-mm-diameter undoped silica rod, so that their axes were parallel to the rod axis. Next, rods with a germanium oxide-doped core were inserted into the holes. The rods were produced from preforms prepared by chemical vapour deposition. The preform assembly thus obtained was consolidated and drawn into optical fibre. A cross-sectional electron micrograph of the MCF is presented below (Fig. 4). The core–cladding refractive index difference was 0.0055, the centre-to-centre distance between neighbouring cores was 47 μm, and the outer diameter of the silica cladding was 180 μm. The measured cutoff wavelength of the first higher mode in the cores ranged from 1340 to 1380 nm.

The loss at a wavelength of 1.55 μm was 0.8 dB km^{-1} in the central core of the MCF and 2.1 to 2.4 dB km^{-1} in the lateral cores. The high level of losses in the lateral cores was caused by the insufficient silica cladding thickness. As a result, some of the light leaked out of the lateral cores to the polymer coating, whose refractive index exceeded that of silica glass. The high optical loss in the lateral cores can be reduced by increasing the spacing between the lateral cores and the outer surface of the silica cladding. Nevertheless, the level of optical losses obtained here is already acceptable for the purposes of this study. The optical cross-talk between the central and lateral cores in a 1560-m-long section of the MCF was measured to be -54 ± 2 dB.

4. Measurement of the group delay difference between the MCF cores

Because of random fluctuations in preform parameters, the cores of an MCF may also differ slightly in parameters. This may lead to mode group index differences between neighbouring cores and, hence, to signal delay time differences between the cores of a given MCF segment. Moreover, differences in parameters between neighbouring cores may be caused by fibre bends. To assess the influence of these factors, we measured the delay time difference between neighbouring cores in the MCF fabricated in this study.

We used an interferometric method, with a Mach–Zehnder interferometer and low-coherence light source. Figure 2 shows a schematic of the experimental setup. The output of a superluminescent semiconductor diode (*1*) with a bandwidth of 50 nm and centre wavelength of 1530 nm was split by a fibre coupler (*2*) between two single-core fibre segments (*3*, *4*). The output end facet of fibre *3* was butt-coupled to one of the

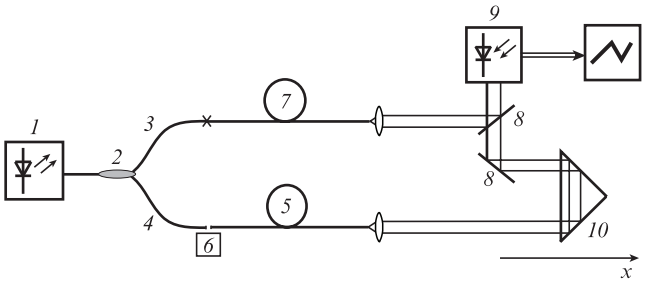

Figure 2. Schematic of the experimental setup used to measure the group delay difference between the MCF cores.

Table 1. Group delay differences $\Delta\tau_{k-0}L^{-1}$/ps m^{-1} between the central and lateral cores per metre of the MCF at different winding radii.

R/mm	Core no., k						Calculated maximum $\Delta\tau_{k-0}L$ values/ps m^{-1}
	1	2	3	4	5	6	
25	0.78	6.07	5.22	−0.89	−6.10	−5.18	9.20
80	0.41	0.79	0.47	−0.34	−0.89	−0.48	2.87
160	0.47	1.08	0.67	−0.35	−1.08	−0,65	1.44

cores of the MCF (*5*) using a three-axis translation stage (*6*). Fibre *4* was fusion-spliced to a single-core fibre segment (*7*) whose length was almost equal to that of the MCF under study (*5*). The light emerging from fibre *7* and the given core of the MCF (*5*) was converted into parallel beams by lenses. The two beams then arrived at a beam-splitting plate (*8*), where they were combined together. After the plate (*8*), the light entered a photodetector (*9*), which was used to find out whether there was interference of the two beams that had passed through the two arms of the interferometer. Interference was observed if the difference between the interferometer arm lengths was smaller than the coherence length of the source used, which was about 50 μm in this study.

To measure the delay time difference between the MCF cores, one of the cores was inserted into the sample arm of the interferometer. Next, moving the roof-mirror reflector (*10*) along the x axis, we varied the sample arm length in the interferometer to reach the interference condition. After that, another MCF core was inserted into the sample arm of the interferometer and the interference condition for this core was also reached. From the difference in the position of the reflector, Δx, which corresponded to the difference between the lengths of the interferometer sample arm, $2\Delta x$, we determined the delay time difference $\Delta\tau$ between the cores:

$$\Delta\tau = 2\Delta x\, n_{\text{air}}/c, \tag{1}$$

where $n_{\text{air}} \approx 1$ is the group index of air. The delay time difference between the other MCF cores was determined in a similar manner.

The group delay difference was measured for a 94-m-long MCF segment wound onto spools of 28, 80 and 160 mm radius. The measured delay time differences between the central and lateral cores per metre of the MCF are presented in Table 1. Figure 3 illustrates the mutual arrangement of the cores differing in delay time difference at an MCF winding radius of 25 mm. Three lateral cores have a negative group delay difference relative to the central core (the group delay in the lateral cores is smaller than that in the central core), and the other three have a positive group delay difference. The absolute values of the delay time difference with opposite signs coincide pairwise to within 15%: the cores with negative values are located on one side from the y axis, and those with positive values, on the other side. Similar delay time distributions over the cores were obtained at MCF winding radii of 80 and 160 mm. Note that the delay time differences in the core pairs differed by up to 34%.

The obtained delay time differences between the cores are caused by MCF bending. Figures 4a and 4b show a straight MCF and the corresponding refractive index profile along the x axis, and Fig. 4c shows a bent seven-core MCF. A bent fibre is optically equivalent to a straight fibre with a tilted refractive index profile [8]. The equivalent x-axis refractive index

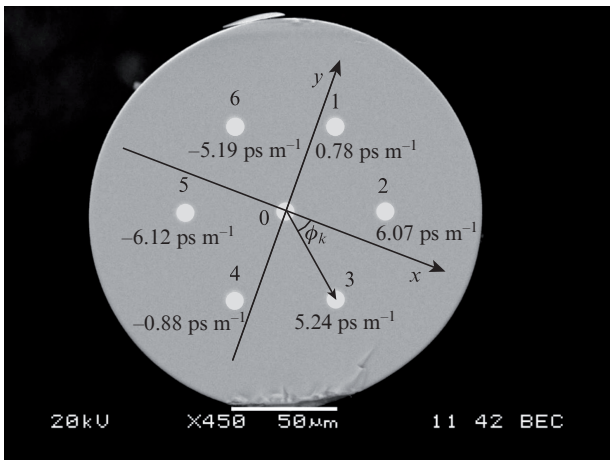

Figure 3. Cross-sectional micrograph of the MCF illustrating the mutual arrangement of the cores (0–6) differing in group delay difference (numbers at the cores) at an MCF winding radius of 25 mm.

profile corresponding to a bent MCF is shown in Fig. 4d. As seen in Figs 4b and 4d, MCF bending will change the phase ($n_{\text{eff}k}$) and, hence, group ($n_{\text{g}k}$) effective refractive indices of core modes and their difference. If the cores are identical, the mode phase indices of the central and lateral cores are related by [9]

$$n_{\text{eff}k} = n_{\text{eff}0}[1 + (D/R)\cos\phi_k], \tag{2}$$

where D is the centre-to-centre distance between neighbouring cores and ϕ_k is the angle between the radial bending direction (x axis) and the radius vector to the centre of the kth core (Fig. 3). Since the mode group index is $n_{\text{g}k} = n_{\text{eff}k} - \lambda\,\mathrm{d}n_{\text{eff}k}/\mathrm{d}\lambda$, we find using (2) that the mode group index difference between the central and lateral cores is

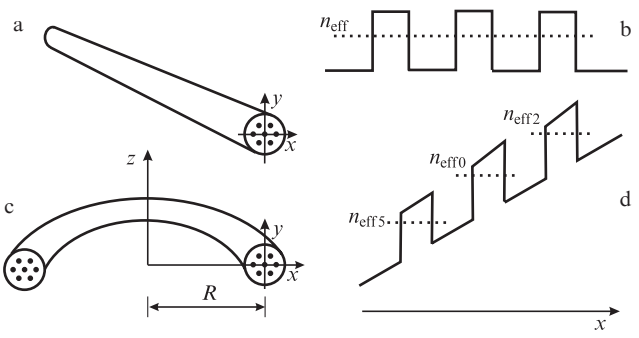

Figure 4. (a) Straight MCF, (b) x-axis refractive index profile of the straight MCF, (c) bent MCF and (d) equivalent x-axis refractive index profile of the bent MCF.

$$\Delta n_{gk-0} = n_{gk} - n_{g0} = \frac{D\cos\phi_k}{R} n_{g0}. \quad (3)$$

The delay time difference between the central and lateral cores is

$$\Delta\tau_{k-0} = \tau_k - \tau_0 = \frac{L}{c}\Delta n_{gk-0} = \frac{L}{c}\frac{D\cos\phi_k}{R} n_{g0}. \quad (4)$$

It is the dependence of the mode group index on ϕ_k that accounts for the experimentally determined $\Delta\tau_{k-0}$ distribution.

The distribution of the measured delay time difference between the central and lateral cores indicates that it is due to MCF bending. Relation (4) can be used to calculate the maximum group delay difference, corresponding to $\cos\phi_k = 1$. In doing so, we take $n_{g0} = 1.468$ (the mode group index of SMF-28 standard telecom fibre). The $\Delta\tau_{k-0}/L$ values calculated for $D = 47$ μm and different bend radii are presented in Table 1. The experimentally measured delay time differences are smaller than the maximum possible value. This is due to the nonzero ϕ_k value. At the MCF length of 1300 m used in the delay line, the optical signal delay difference between the cores is less than 12 ns at an MCF bend radius of 25 mm, less than 4 ns at a bend radius of 80 mm and less than 2 ns at a bend radius of 160 mm. These values are far less than the signal delay (6.36 μs) after propagation through one MCF core and, hence, the fibre bending-induced change in the group delay difference between the MCF cores will have no significant effect on the parameters of the FODL configuration under study.

5. Light input/output device for the MCF fibre

To couple light into one of the MCF cores and then couple it out of the core and into a single-core fibre, we used a small fibre-optic device [10] that ensured sufficient mechanical reliability and low optical losses. The input/output device configuration chosen had the form of seven single-core fibre segments stacked together. On one side of each fibre segment, its polymer coating was stripped over a length of several centimetres and then the silica cladding in the stripped portion of the fibre was etched away with hydrofluoric acid to a diameter equal to the centre-to-centre distance between neighbouring cores in the MCF. After that, the etched portions of the fibre were stacked together and inserted in a silica capillary tube whose inner diameter was three times the overall diameter of the etched fibres. The fibre sections in the capillary tube were glued up and the end face of the tube was polished. The polished end face of the input/output device is shown in Fig. 5a. The geometry of the arrangement of the single-core fibre cores corresponded to the arrangement of the cores in a cross section of the MCF. Next, the end faces of the input/output device and MCF were butt-joined and aligned, following which the end faces were glue-spliced. The splice was secured in a larger diameter capillary tube, which was also made of silica. Figure 5b shows the input/output device and the MCF spliced to it. The optical losses due to MCF splicing to input/output devices is indicated in Table 2. The level of optical losses thus achieved allowed us to carry out optical signal delay experiments.

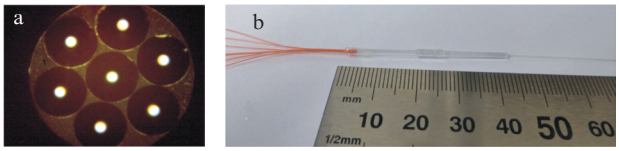

Figure 5. (a) End face and (b) appearance of the input/output device.

6. Experimental results and discussion

Figure 6 shows a combined oscilloscope trace of pulsed microwave signals at the PD output after they passed through one, two and more MCF cores in the configuration schematised in Fig. 1. The numbers at the pulses specify the number of cores the signal passed through. Also shown in Fig. 6 are synchronisation pulses (SPs) provided directly by the SG. Because of the optical loss (Table 2), increasing the number of cores the signal passed through was found to reduce the voltage amplitude of the electric signal at the photodetector output. To compensate for the loss, an erbium-doped fibre amplifier (A) (Fig. 1) was placed between the third and fourth cores in the FODL. For all the channels to be identical in length, the lengths of the lead-in single-core fibres were chosen with allowance for the amplifier length. To this end, additional turns T1–T7 were used, whose lengths were equal to the amplifier length. Because of the high optical loss and the presence of the amplifier, the signals in Fig. 6 differ in amplitude. The optical losses indicated in Table 2 can be substantially reduced in future work by improving the MCF and IO device fabrication processes.

The maximum delay, after the signal passed through all the MCF cores, was 45.0 μs (Fig. 6, trace 7), as measured on the leading edge of the pulse. The optical delay difference between neighbouring channels was 6.43 μs. The optical delays obtained correspond to values calculated as $\tau = (Ln_g)/c$. At $n_g = 1.468$ and $L = 1300$ m, the calculated group delay is 6.36 μs. The discrepancy between the calculated and measured delay differences between the channels in the scheme under consideration is due to the additional length of the erbium-doped fibre amplifier and the turns T1–T7 of the lead-in single-core fibres.

Table 2. Optical losses in the FODL at a wavelength of 1.55 μm.

Loss	Core no.						
	0	1	2	3	4	5	6
Loss in the MCF (1.55 μm) /dB km^{-1}	0.8	2.1	2.2	2.4	2.2	2.3	2.3
MCF–IO1 splice loss/dB	0,8	1.6	1.3	1.5	1.4	1.8	1.7
MCF–IO2 splice loss/dB	0,9	0,6	0.6	1.1	1.6	0.6	0.5
Total loss/dB	2.5	4.4	4.1	4.8	5.2	4.6	4.4

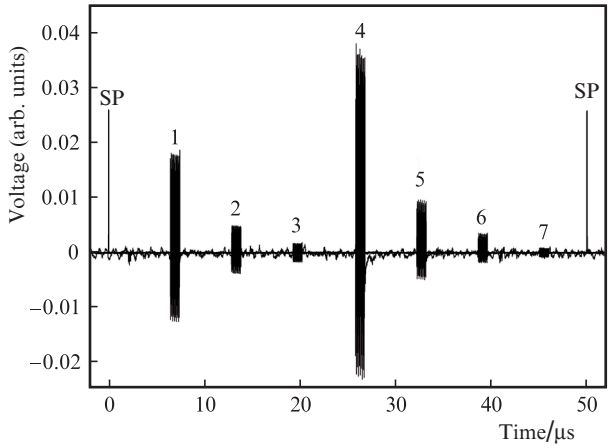

Figure 6. Combined oscilloscope trace of pulsed microwave signals at the photodetector output after they passed through one, two and more MCF cores, and synchronisation pulses (SPs) from the SG.

7. Conclusions

In this work, we have demonstrated the first switchable fibre-optic long-delay line based on a 1300-m-long multicore optical fibre. Using the delay line, we have obtained signal delay times of up to 45 μs at 6.43-μs intervals. The proposed fibre-optic delay line configuration is potentially attractive for applications where considerable signal delay times are needed. Sequential signal propagation through the cores of a multicore optical fibre makes it possible to reduce the optical fibre length necessary for obtaining a required signal delay and, hence, the weight and dimensions of signal delay devices, which is of particular importance for on-board applications of such devices.

Acknowledgements. This work was supported by the RF Ministry of Education and Science (Project No. RFMEFI60715X0138).

References

1. Seeds A. *IEEE Trans. Microwave Theory Tech*., **50**, 877 (2002).
2. Capmany J., Novak D. *Nat. Photonics*, **1**, 319 (2007).
3. Capmany J., Ortega B., Pastor D., Sales S. *J. Lightwave Technol*., **23**, 702 (2005).
4. Minasian R.A. *IEEE Trans. Microwave Theory Tech*., **54**, 832 (2006).
5. Inao S., Sato T., Sentsui S., Kuroha T., Nishimura Y., in *Proc. Opt. Fiber Commun.* (Washington, D.C., USA, 1979) WB1.
6. Egorova O.N., Astapovich M.S., Belkin M.E., Semenov S.L. RF Patent Application No. RU 2016124251, 20 June 2016.
7. Ishida I., Akamatsu T., Wang Z., Sasaki Y., Takenaga K., Matsuo S., in *Proc. Opt. Fiber Commun.* (Anaheim, CA, 2013) OTu2G.
8. Marcuse D. *Appl. Opt*., **21**, 4208 (1982).
9. Li S., Butler D.L., Li M.-J., Koklyushkin A., Nazarov V., Khrapko R., Geng Y., McCollum R.L., in *Proc. IEEE Photonics Conf.* (Bellevue, WA, 2013) TuF3.2.
10. Li B., Feng Z., Tang M., Xu Z., Fu S., Wu Q., Deng L., Tong W., Liu S., Shum P.P. *Opt. Express*, **23**, 10997 (2015).